Paper No.
08068

12th Middle East Corrosion Conference & Exhibition

Surface Modification of Al Alloy 2014 by Electrochemical Deposition of Ni

Anwar UI-Hamid
King Fahd University of Petroleum & Minerals P. O. Box 1073
Dhahran 31261, Saudi Arabia
Fax: +966-3-8603996
E-mail: anwar@kfupm.edu.sa

Abdul Quddus
King Fahd University of Petroleum & Minerals
Dhahran 31261, Saudi Arabia
E-mail: amguddus@kfupm.edu.sa

Abdulrashid I. Muhammad
King Fahd University of Petroleum & Minerals
Dhahran 31261, Saudi Arabia
E-mail: arashid@kfupm.edu.sa

Luai M. AI-Hadhrami
King Fahd University of Petroleum & Minerals
Dhahran 31261, Saudi Arabia
E-mail: luaimalh@kfupm.edu.sa

ABSTRACT

The surface of Aluminum alloy AA 2014 was modified by electrochemical deposition of Ni and its effect on corrosion performance was evaluated. Standard Watt's bath with varying potential, current and time was employed for deposition. The Ni-coated samples were heat treated to improve coating characteristics. Corrosion behavior was studied by electrochemical testing and microstructural characterization was performed using scanning electron microscopy. Microhardness was also undertaken. Experimental results indicate that electrochemical deposition combined with heat treatment can be used to improve the surface properties of Al alloys.

1. INTRODUCTION

Aluminum exhibits outstanding chemical stability under most atmospheric conditions due to the rapid formation of a thin (≈1nm) protective layer of alumina (Al_20_3) at its surface. Since, however, pure Al lacks adequate mechanical strength for structural applications, it is combined with various alloying elements and heat treated to produce grades with desired properties. On the other hand, most alloying elements tend to lower the corrosion resistance of AI. Both degree and nature of the corrosion attack are greatly influenced by thermal treatment and the nature of alloy surface. To enhance corrosion performance, the surface of a high-strength Al alloy is generally coated with cladding, anodizing and/or other protective layers. There is a need for new surface protection systems with better combined mechanical strength and corrosion resistance to meet the demands of aggressive operating conditions.

Copper is a well known alloying element in high-strength Al alloys. Other alloying elements such as Mg and Si in addition to some Cr and Mn are also present as demonstrated by the 2014 alloy grade. Alloy 2014 is a heat treatable alloy with high fatigue strength and is used in high strength structural applications such as aircraft fittings and wheels, military vehicles and bridges, forgings for trucks and machinery, weapons manufacture, etc. However, Al 2014 exhibits poor corrosion resistance in marine atmospheres and sea water, thereby requiring additional surface protection. Protective coatings also serve to improve alloy wear performance. Various techniques are employed for surface modification including plasma and spray coating, welding, electrolytic and electroless coating, etc. Electrolytic and electroless coating are competitive techniques with certain advantages associated with each one of them. Electroless plating is usually more expensive than electroplating, and takes longer to achieve a given thickness of coating deposit with accompanying waste disposal problems[1,2]. The present study was undertaken to assess the use of electrolytic deposition for Ni plating of Al alloys. Ni coating is extensively used in industry to improve the surface properties of Al alloys for applications such as Al automotive parts, wrought products, castings, memory disks, connectors, etc. Nickel plating protects aluminum from hostile environments and makes a hard, wear-resistant surface that allows aluminum to be used for applications not otherwise suitable. Nickel coatings may also have a pleasing appearance thereby satisfying decorative needs along with functional requirements.

The adhesion of protective coatings is adversely affected by the presence of copper in Al 2014 due to galvanic effect. The difference in the electrical conductivity between the $CuAl_2$ particles and the alloy matrix produces an inhomogeneous electric field resulting in defects within deposited layer during electrodeposition process [3]. The presence of cathodic Cu-rich second phase particles also affects the thickening rate of coating at localized regions resulting in inhomogeneous growth [4]. Due to these reasons, the adhesion of electrodeposited coating is adversely affected. In the present study, electrodeposition was performed using constant current (Galvanostatic) as well as constant potential (Potentiostatic) methods. Thermal treatment of electrodeposited samples was conducted to improve adhesion. Corrosion behavior of coated alloys was determined using electrochemical corrosion tests. The morphologies, microstructures and compositions of the coatings were characterized using scanning electron microscopy coupled with energy dispersive X-ray spectroscopy. Mechanical strength was evaluated using surface and microhardness measurements. The aim of this study was to determine the conditions under which uniform, compact and adherent Ni coatings can be obtained on Al alloys using electrochemical techniques.

2. EXPERIMENTAL PROCEDURE

2.1. Materials

The nominal composition of the Al alloy used in this study is given in the table below.

Elements	Al	Cu	Fe	Mn	Si	Mg	Zn	Ti	Cr
Chem. Comp. (Wt.%)	Bal.	4.4	0.5	0.8	0.8	0.4	0.25	0.15	0.10

2.2. Electrodeposition

The samples were metallographically prepared to two surface finishes, e.g., 600 grit size and 1 μm diamond polished. They were degreased with acetone and rinsed with distilled water. The samples were then pretreated by dipping in zincate solution for 30 seconds followed by a vigorous rinse in a solution of methanol (97%) and HNO_3 (3%) to produce a shining surface. Finally, the samples were dipped in zincate solution again for one second and introduced into Watt's plating solution immediately afterwards. The composition of Watt's bath and zincate solution used in this study is given below:

Material	Amount
Watt's bath	
Nickel sulfate (g)	125
Nickel chloride (g)	22
Boric acid (g)	15
Distilled water (l)	0.5
Zincate solution	
Sodium hydroxide (g)	263
Zinc oxide (g)	50
Ferric chloride (g)	0.5
Potassium sodium tartrate (g)	5
Distilled water (l)	0.5

Anode (Ni) and Cathode (Al 2014) of the plating cell were connected to the Potentiostat/Galvanostat and Nickel was deposited onto the Al 2014 by selecting the appropriate current or voltage for a predetermined period of time. Optimal plating results were obtained when the Watt's solution was maintained at a temperature of 45 °C with slow stirring of approximately 80 rpm and a pH level of 3.6.

2.3. Heat Treatment

In the first phase of heat treatment, selected Ni-coated samples were heated to 525 °C for 10 hours in a tube furnace under argon atmosphere followed by water quenching. The second phase of heat treatment consisted of an aging process where the samples were heated to 170 °C for 10 hours under argon atmosphere followed by furnace cooling in the cold zone.

2.4. Corrosion Measurements

Corrosion tests were carried out with corrosion console model EG&G 350 in 3.5 wt% NaCl solution using Tafel technique. The morphology of surface damage induced as a result of corrosion tests was studied using SEM.

2.5. Microstructural Characterization

The Ni deposited samples were metallographically mounted in cross-section, ground with 600 grit size SiC paper and polished using 1 μm diamond paste. They were then covered with a thin layer of carbon using a carbon evaporator making the surface electrically conducting to avoid charge build-up during SEM analysis. Top surfaces were analyzed in an as-received condition. A scanning electron microscope (SEM) coupled with energy dispersive spectroscopy (EDS) was used to examine the samples. The Si(Li) EDS detector was equipped with an atmospheric thin window capable of detecting elements down to Be. The accelerating voltage of SEM was maintained at 20keV during analysis and imaging was performed using both secondary and backscattered electrons. Vickers microhardness tests were undertaken to determine the hardness of coatings.

3. RESULTS AND DISCUSSION

The microstructure of an uncoated etched sample of Al 2014 is shown as an example in Figure 1a. Secondary phase particles with a size range of ≈1-5 μm were observed both within the matrix and at alloy grain boundaries. Microchemical analysis using SEM/EDS indicated that the major elemental constituents of these particles were Al and Cu as demonstrated in the example of Figure 1b. Quantification of the spectral data revealed a composition with 40.5 wt% Al and 59.5 wt % Cu

consistent with the second phase particles of $CuAl_2$. A particle of $CuAl_2$ acts as a local cathodic region with respect to the surrounding matrix which becomes anodic due to its depletion in Cu. As a result, a galvanic couple is established promoting electrochemical corrosion. In addition, local galvanic cells associated with the precipitation of $CuAl_2$ particles also result in pitting damage when exposed to solution containing chlorides. In view of above, in addition to improving mechanical properties, the susceptibility of Al 2014 alloy to corrosion necessitates the use of surface protection by effective coatings.

The morphologies of Ni coatings formed at the surface of Al 2014 alloy at different deposition conditions are discussed below. All samples were polished to 1 μm surface finish except where specifically mentioned. Potentiostatic method using a constant potential of 1.2V for 2 minutes resulted in a discontinuous deposition as shown in Figure 2a. Large areas of alloy surface remained exposed showing no Ni deposition. A higher magnification micrograph shown in Figure 2b revealed a relatively fine and smooth morphology of the Ni deposit. Deposition time of 10 minutes under the same conditions revealed a thicker deposit with more defined grain morphology as shown in Figure 2c. Some areas of the alloy surface are covered with a thick film as shown in Figure 2d. The EDS spectrum obtained from this areas showed primarily Al and O in addition to Ni and S (see Figure 2e). Non-uniform nature of deposition is evident from cross-sectional view of the sample shown in Figure 2f.

Secondary electron SEM image of the deposit obtained using galvanostatic method with 25 mA/cm^2 of current density shows sub-micron grain size and an faceted morphology in Figure 3a. The deposition was not completely homogeneous revealing localized regions of exposed alloy surface. The sample with a 600 grit size surface finish failed to produce substantial Ni deposit at a current density of 50 mA/cm^2 as shown in Figure 3b. Microchemical analysis performed using SEM/EDS revealed that the white outwardly protruding agglomerate was composed of Al, O, S and Ni while the background surface showed the presence of mainly Ni with small amounts of Al and O as shown in Figures 3c and 3d respectively. The Al alloy surface is thought to have oxidized during deposition process to form mainly Al_2O_3 intermixed with some compounds containing S and Ni. The source of S will be $NiSO_4$ from the bath electrolyte.

Best results were obtained by using a constant deposition current density of 50 mA/cm^2 as shown in the secondary electron SEM image of Figure 4a. Relatively uniform and continuous Ni deposit was obtained after 10 minutes of deposition. The deposit showed good adherence and covered almost the entire alloy surface with only a few localized regions at microstructural level showing exposed alloy. The Ni deposit assumes a globular morphology at the start of the process shown as an example in Figure 4b. However, as deposition continues, the globular nature of deposit disappears and is replaced by a more faceted structure as seen in several examples cited above.

The coated Al 2014 alloy was heat treated in order to observe its effect on the morphology and hardness of Ni coating as well as its adhesion to the alloy substrate. The objective was to form intermetallics that would serve to increase the adhesion between the Ni coating and Al alloy substrate by inducing a reaction between the two at an elevated temperature. In order for the Al 2014 substrate to retain its intended mechanical properties, a heat treatment schedule that would allow precipitation of equilibrium $CuAl_2$ phase in Al alloy matrix was followed. It is clear from Al-rich section of Al-Cu phase diagram shown in Figure 5 that Cu has maximum solubility limited to 5.65 wt% at the eutectic temperature of 548 °C and decreases to nearly 0 wt% at room temperature. It can be observed from Figure 5 that any Al-Cu alloy containing up to 5.65 wt% Cu can be heated to the α-phase field, quenched and then aged to precipitate the equilibrium θ-phase ($CuAl_2$) within a matrix of α-phase. In our study, the electrodeposited samples were heat treated at 520 °C for 10 hours and then aged at 170 °C also for 10 hours. The morphology of Ni deposit after heat treatment is shown in the secondary electron SEM images of Figures 6a and b. The grain structure assumes globular nature and deposit adherence showed a marked improvement due to the formation of an intermediate layer between the Ni deposit and underlying substrate as shown in the cross-sectional views of the heat treated sample in Figures 7a and b. The thickness of Ni deposit was more

than 11 μm and that of intermediate layer was 6 μm. Uniform deposition was also observed at regions where relatively coarse $CuAl_2$ particles were intersecting the alloy surface. A higher degree of $CuAl_2$ particles were observed to be precipitated during the heat treatment process. Detachment or spalling of the Ni deposit was not observed at any region of the sample. Composition profile obtained across the deposit thickness starting from the outer edge of the coating towards the Al substrate is shown in the form of a line-scan in Figure 8. The morphology of the intermediate layer as well as the line-scan suggests that Ni diffuses inward into the Al 2014 alloy accompanied by Al diffusion outward. It is likely that they interact to form intermetallics of the type $Al_3(Cu, Ni)_2$, Al_3Ni and Al_2Ni_2 within the intermediate layer [3] as indicated by microchemical analysis obtained at the top and bottom regions of intermediate layer shown in Figures 9a and b respectively. X-ray mapping images of the heat treated sample illustrating the distribution of Al, Ni, Cu, Fe and Mn are shown in Figure 10. Copper was detected within the intermediate layer while the alloy regions immediately beneath the layer were denuded of Cu to 2.4wt%. These regions also showed a lower degree of $CuAl_2$ particles, thought to be consumed during the heat treatment.

Hardness of Al alloy matrix before and after heat treatment was measured as 150 and 70 VHN respectively. The decrease in alloy hardness indicates that the alloy was over-aged during heat treatment. Over-aging is thought to have taken place during relatively prolonged sample cooling within the cold zone of the tubular furnace. The hardness of Al 2014 in the T4 temper is listed in the literature as 120 VHN. Hardness obtained from the top surface of Ni-coating formed on the non-heat treated sample was 230 VHN showing a substantial increase compared to the bulk alloy. The hardness from top surface of the Ni-coating formed on heat treated sample was measured as 70 VHN, showing a considerable decrease compared to the non-heat treated sample. This behavior is similar to that shown by the bulk alloy. Microhardness results indicate that the hardness of the Ni deposit is greater than that of Al 2014 which represents an improvement in latter's surface properties. It was not possible to measure the hardness of the Ni deposits formed on samples mounted in cross-section since the dimensions of the indenter used in hardness tester were larger than the coating thickness. Likewise, it was not possible to evaluate the intermediate layer which is expected to have higher hardness than the top surface of Ni coating. In conclusion, a heat treatment procedure needs to be identified that does not result in a decrease in hardness.

The corrosion behavior of Ni-coated and bare Al 2014 samples was compared by undertaking Tafel tests. Examination of surface morphology using SEM after exposure to NaCl solution using similar polarization conditions showed that bare Al alloy was subjected to a high degree of uniform corrosion (see Figure 11a) and formation of Al_2O_3 at localized regions of alloy surface (see Figure 11b). On the other hand, Ni-coated sample did not reveal any corrosion damage (see Figure 11c). This is consistent with galvanic series table where Al is shown to be slightly anodic to austenitic Ni.

During the course of this study, several trial runs of electrodeposition of Ni on Al 2014 were undertaken using different conditions. It was observed that factors such as bath temperature, rate of stirring, pH level of the electrolyte, level of applied current and potential and nature of alloy surface all influence the nature and adherence of Ni deposit formed on Al alloy surface. Higher than optimal temperature and stirring rate resulted in non-adherent and flaky deposits while lower temperature and stirring led to non-uniform deposition. Increased pH levels of the bath gave rise to cracked, flaky and blackened deposits.

4. CONCLUSIONS

Galvanostatic method produced more adherent and uniform Ni deposits on Al 2014 alloy compared to the Potentiostatic method. Fine surface finish of the alloy surface was found more appropriate for deposition compared to 600 grit size grinding finish. Optimum control of parameters like current, bath temperature, stirring rate, was required to achieve desired coating properties. Heat treatment improved the adhesion of Ni deposit by forming an intermediate layer comprising of Al, Cu and Ni at the alloy substrate. Alloy deposited with Ni showed an improvement in corrosion behavior and

hardness compared to bare Al 2014. Electrodeposition represents a viable method of producing hard and corrosion resistant Ni coatings on Al alloys.

5. REFERENCES

1. D. Pletcher, F. C. Walsh, *Industrial Electrochemistry*, 2nd Edition, Chapman and Hall, London, 1990.
2. J. K. Dennis, T. E. Such, *Nickel and Chromium Plating*, Butterworth, London, 1986.
3. J. M. Molina, R. A. Saravanan, J. Narciso, E. Louis, *Materials Science & Engineering*, A 383, p. 299, 2004.
4. Y. Liu, P. Skeldon, G. E. Thompson, H. Habazaki, K. Shimizu, *Corrosion Science*, Vol. 47, p. 341, 2005.

6. ACKNOWLEDGEMENT

The authors wish to acknowledge the support of Research Institute at the King Fahd University of Petroleum & Minerals, Dhahran, Saudi Arabia.

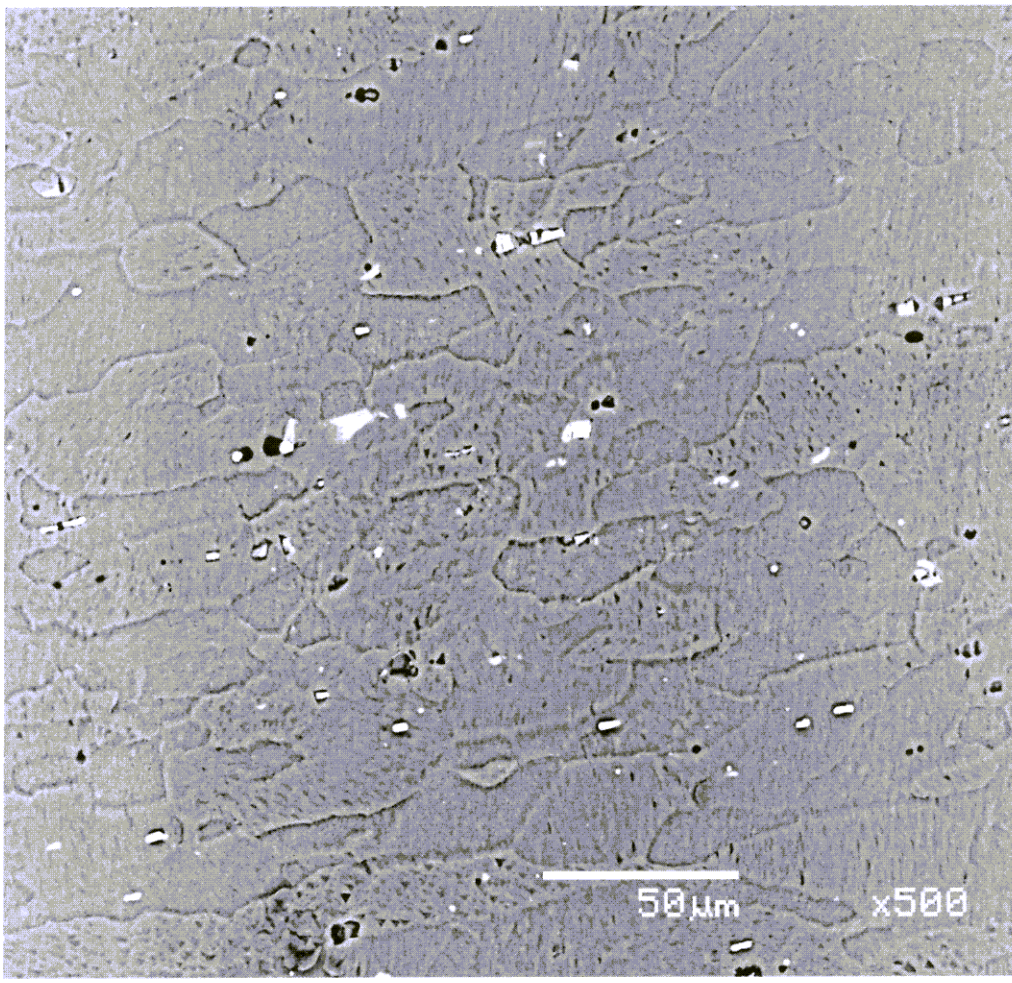

Figure 1a

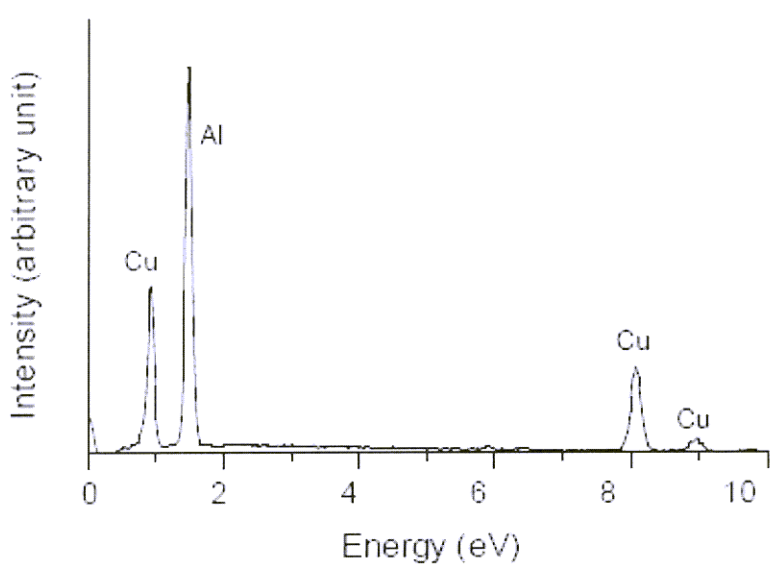

Figure 1b

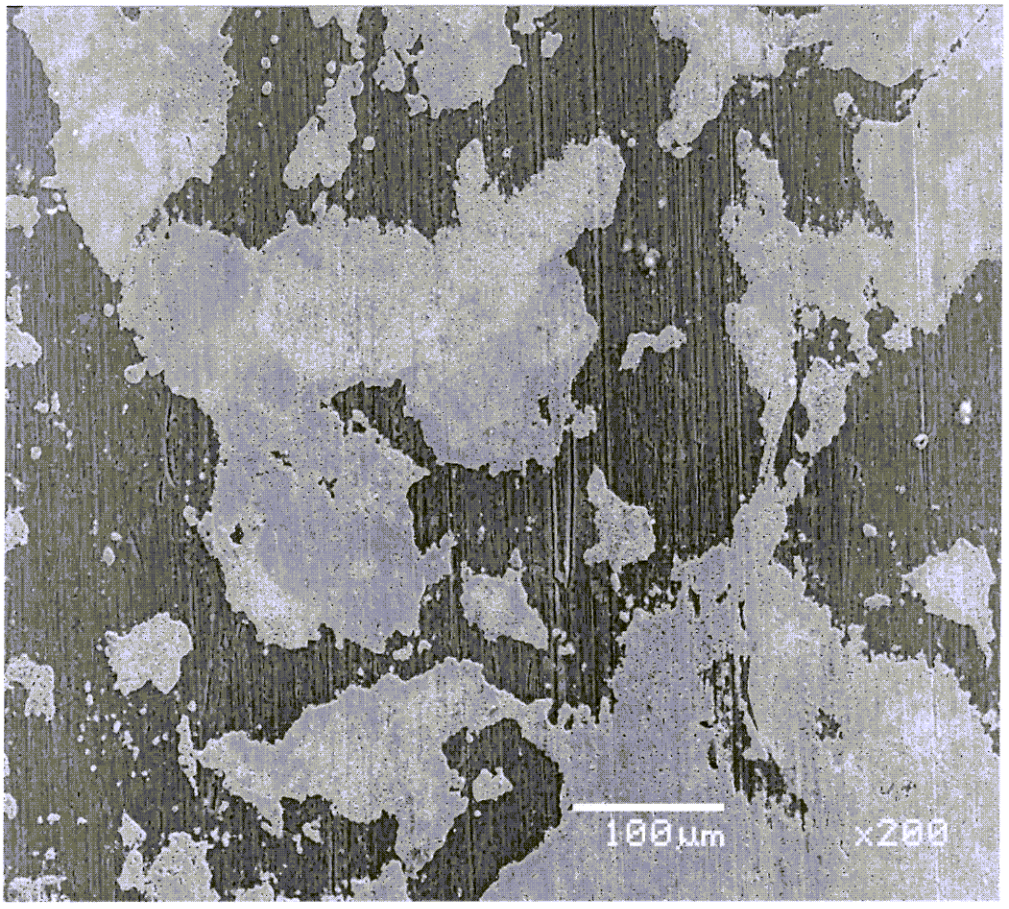

Figure 2a

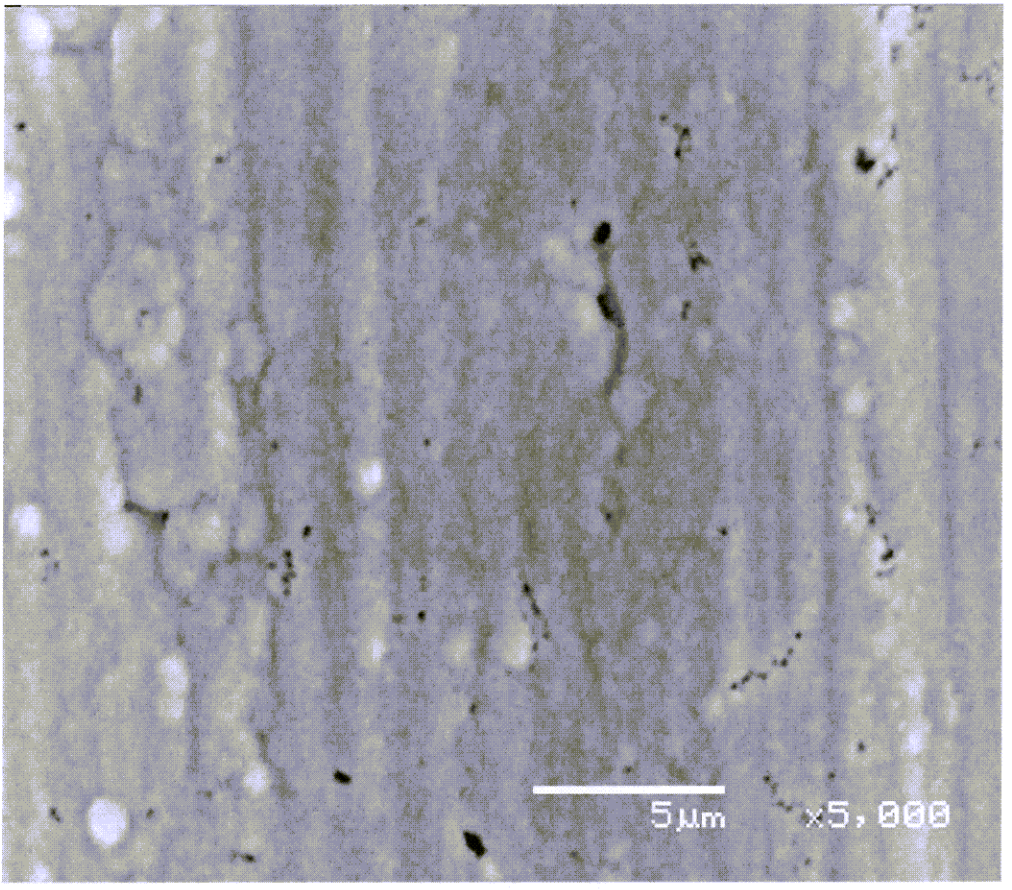

Figure 2b

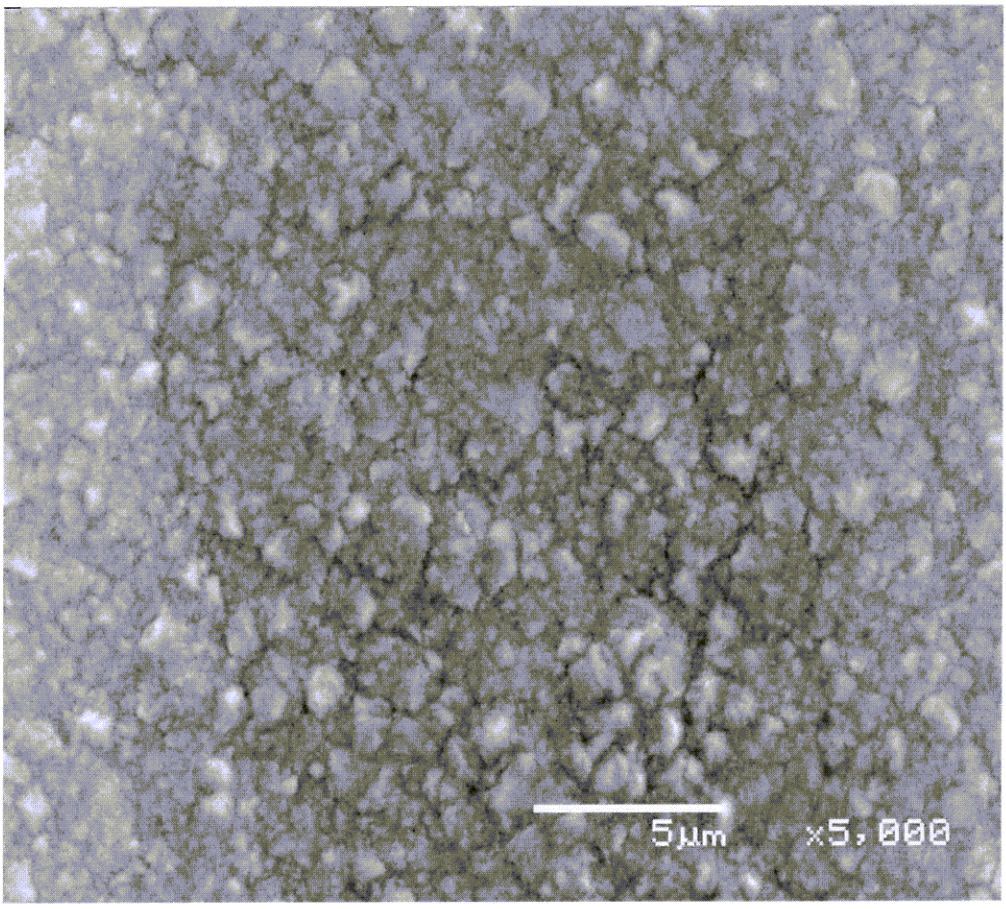

Figure 2c

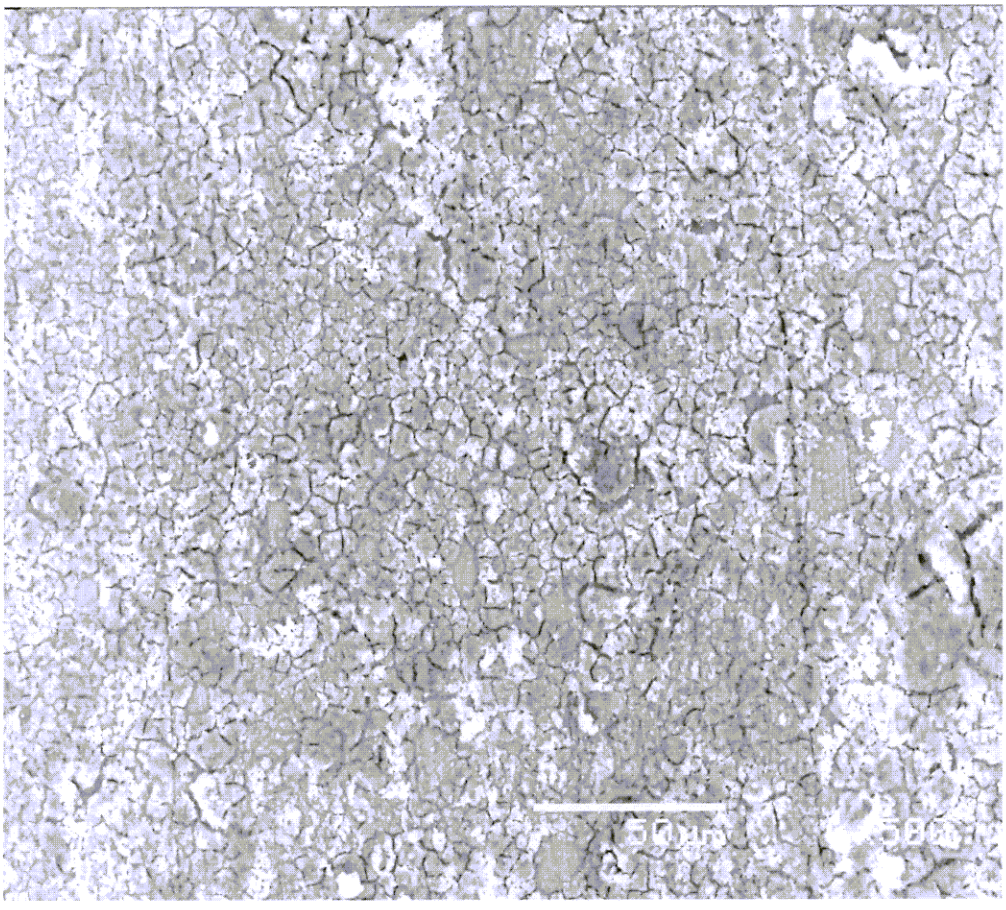

Figure 2d

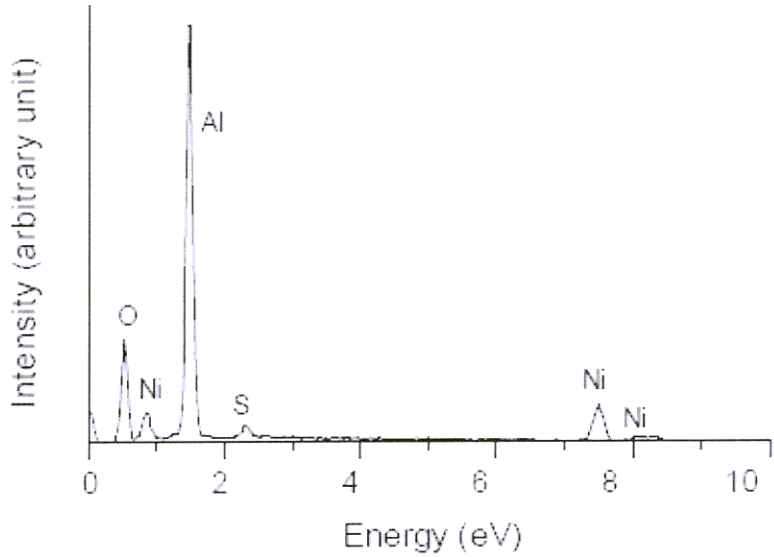

Figure 2e

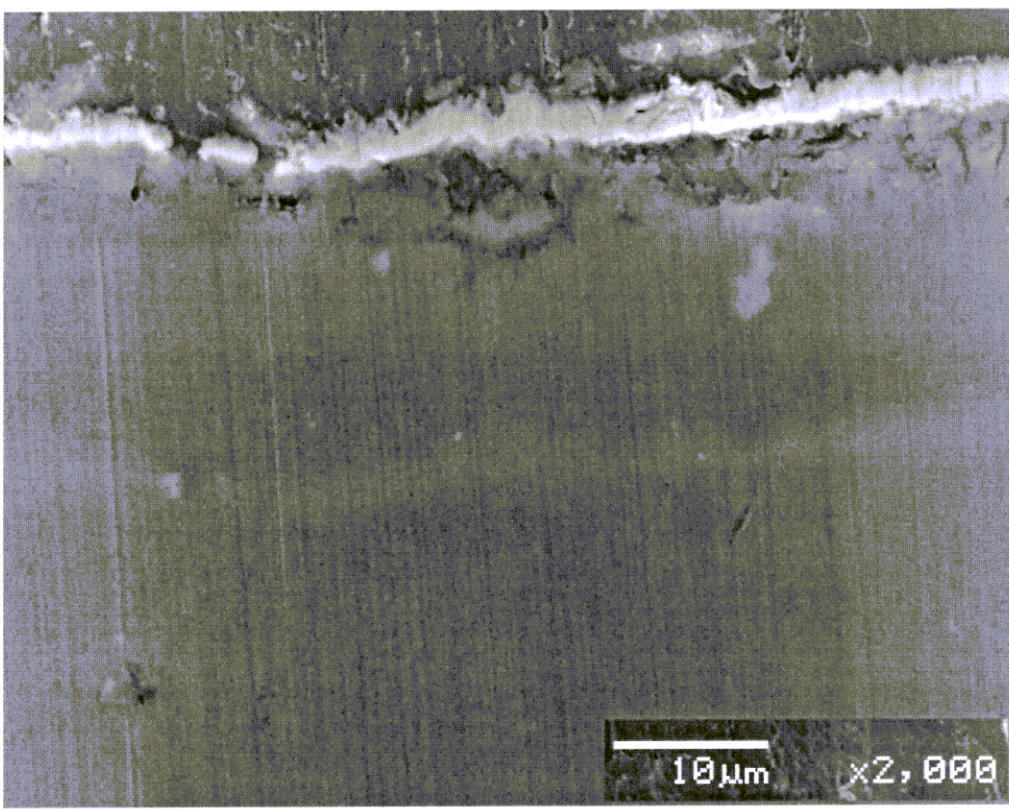

Figure 2f

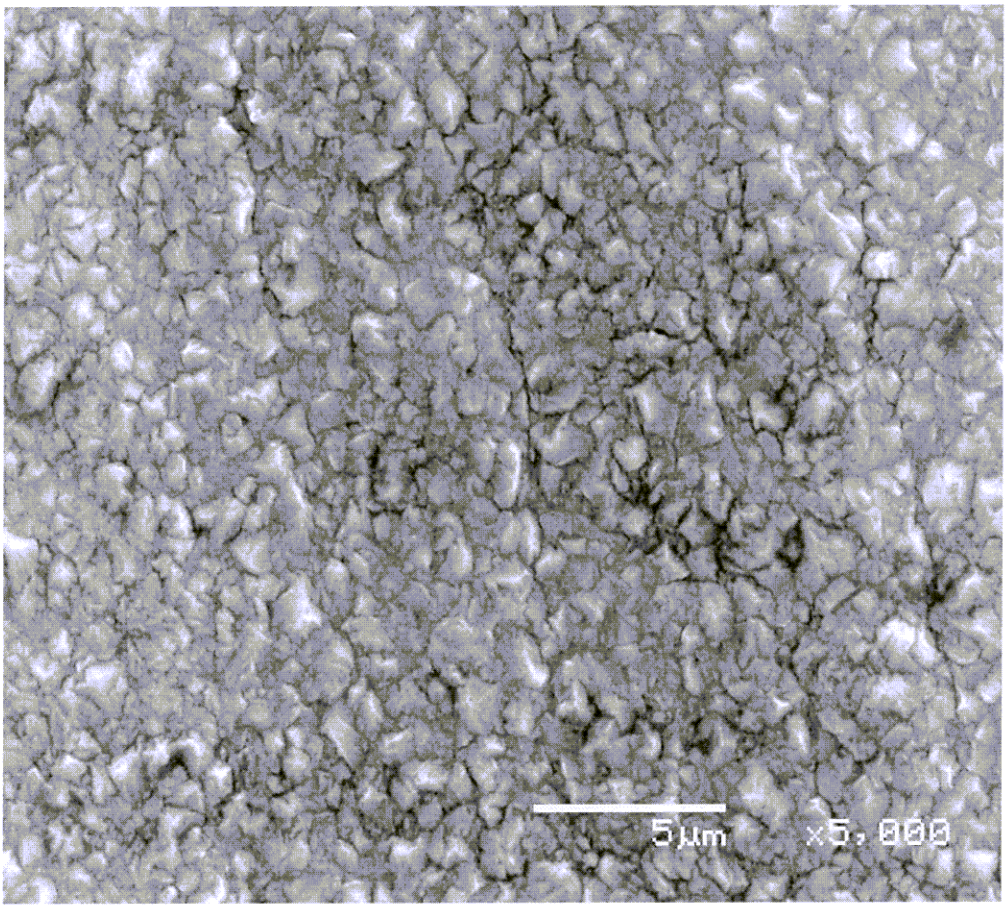

Figure 3a

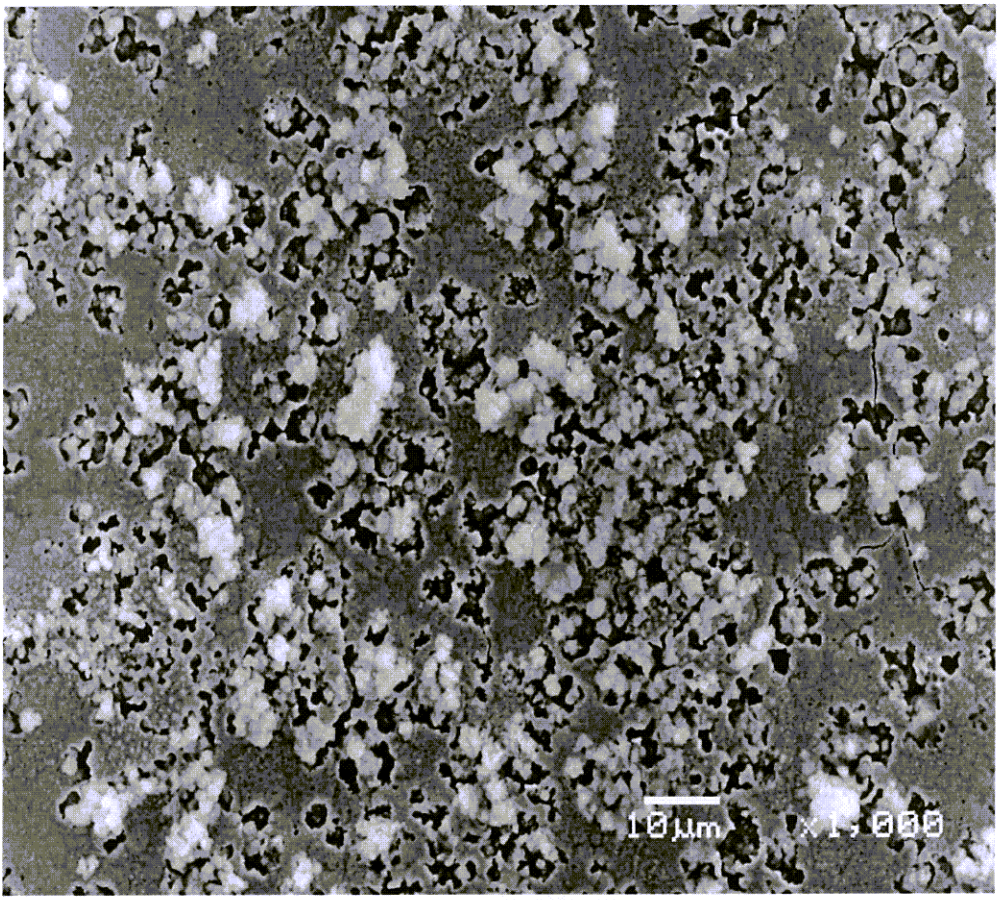

Figure 3b

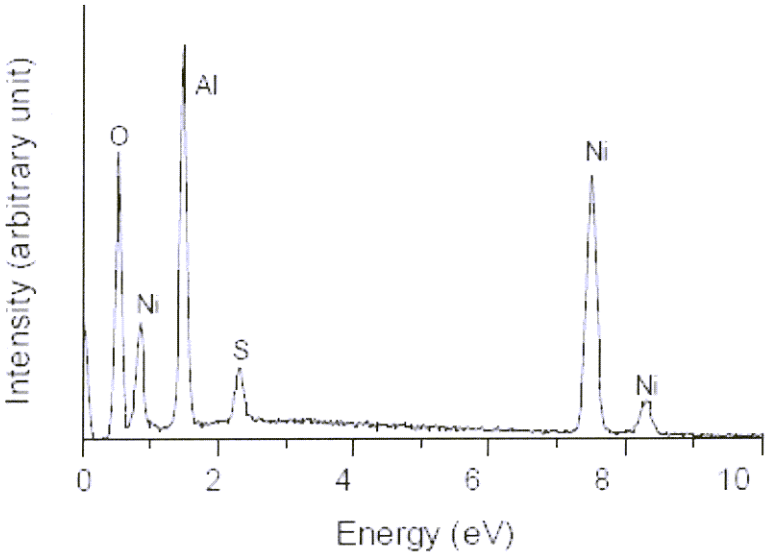

Figure 3c

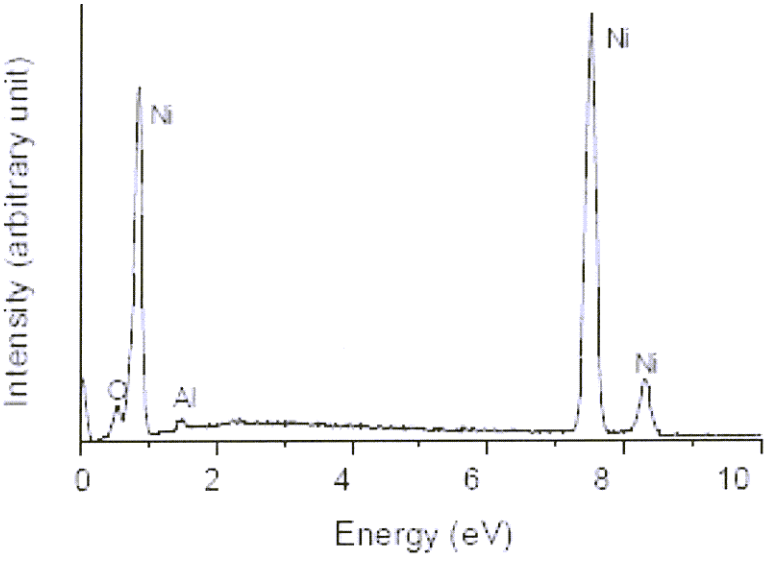

Figure 3d

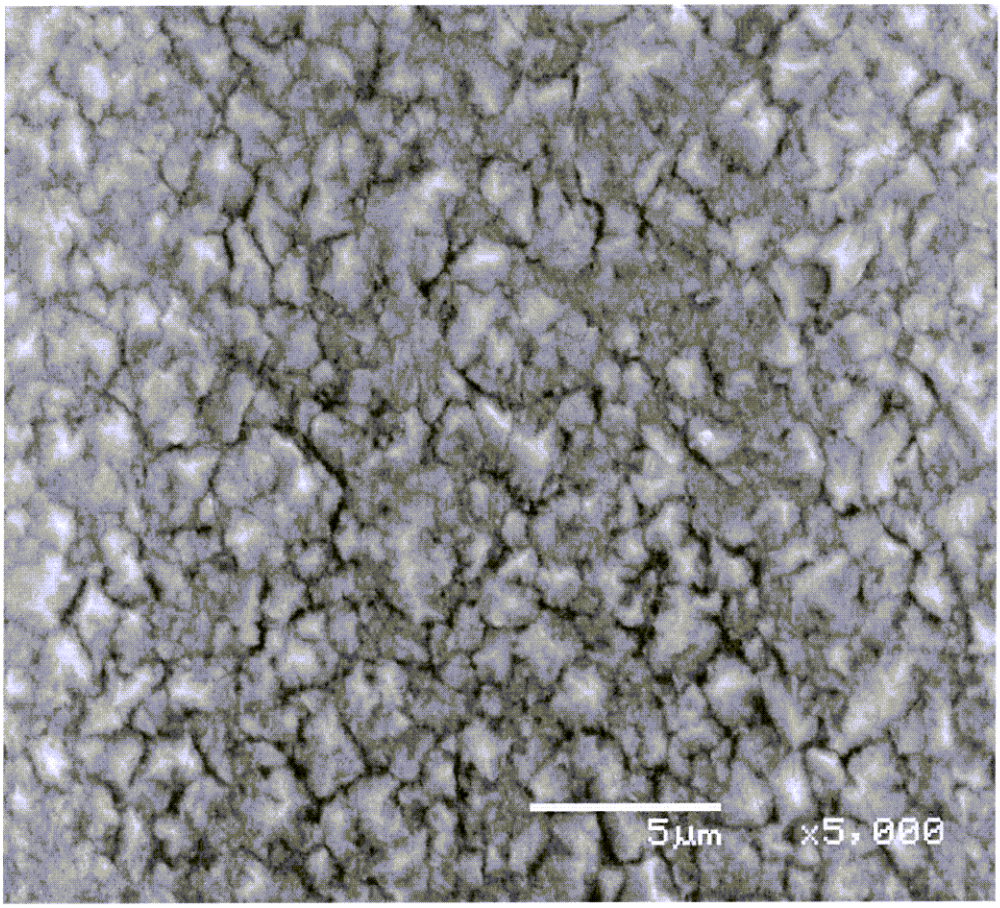

Figure 4a

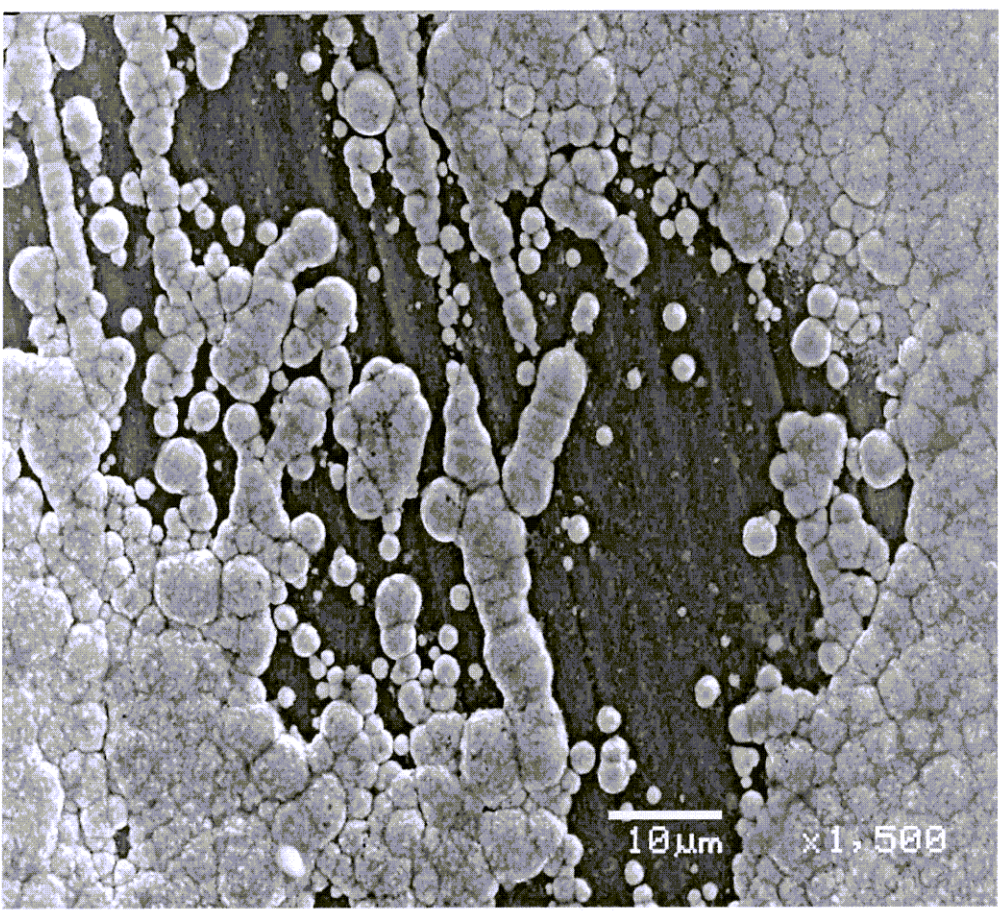

Figure 4b

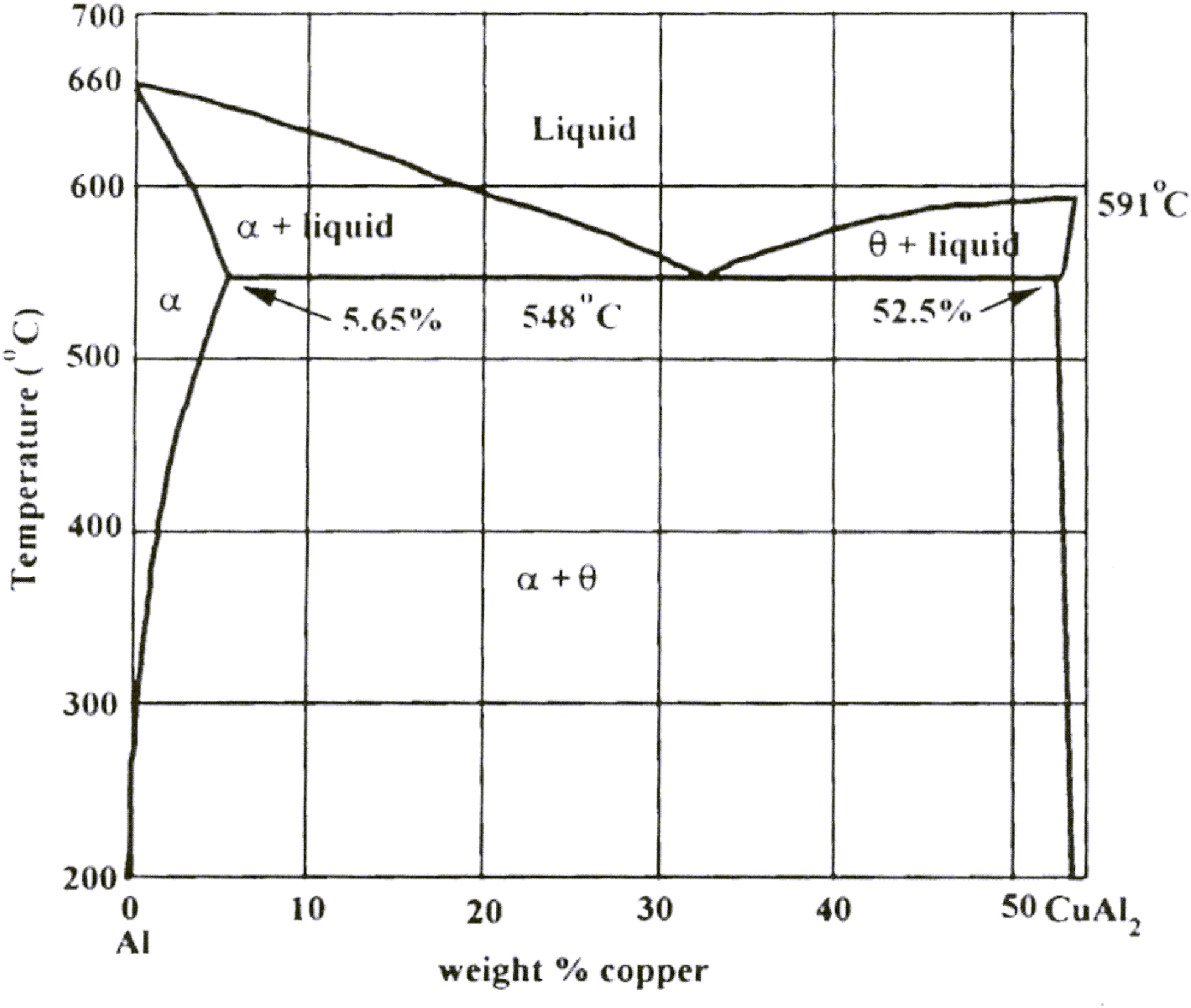
700
660
600
500
400
300
200
Liquid
α + liquid
θ + liquid
591°C
α
5.65%
548°C
52.5%
α + θ
Temperature (°C)
0
Al
10
20
30
40
50 CuAl2
weight % copper

Figure 5

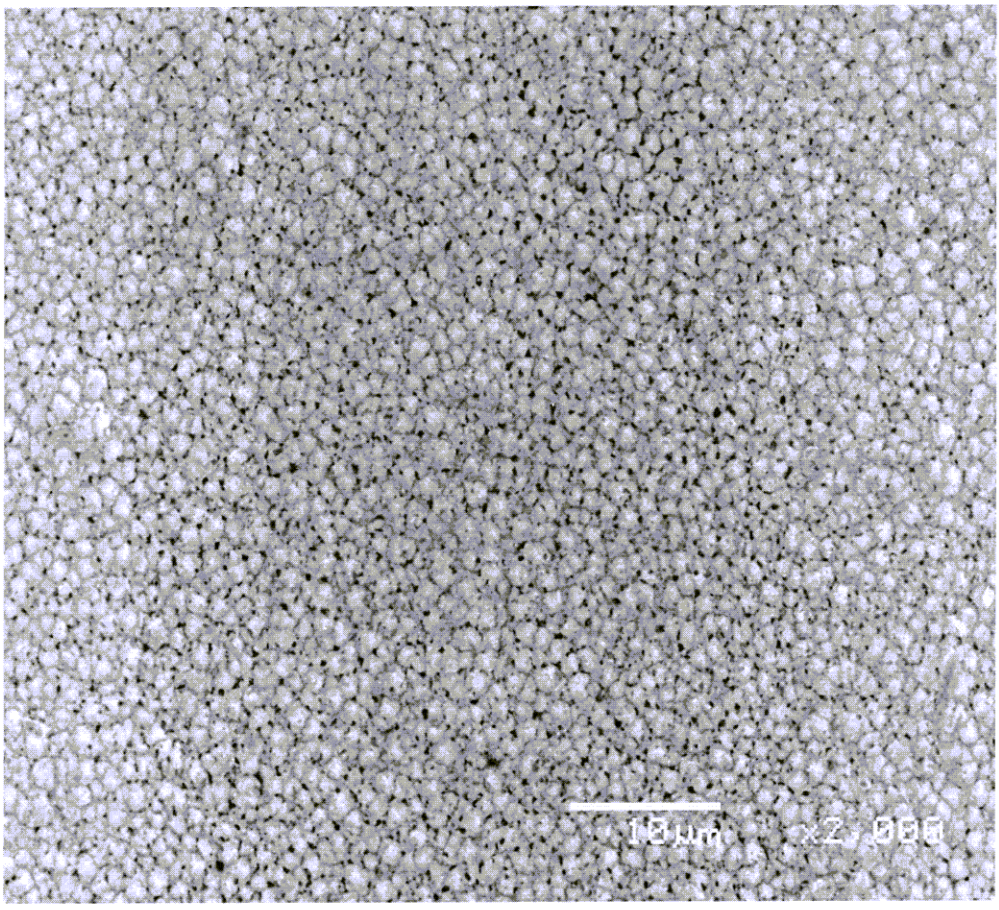

Figure 6a

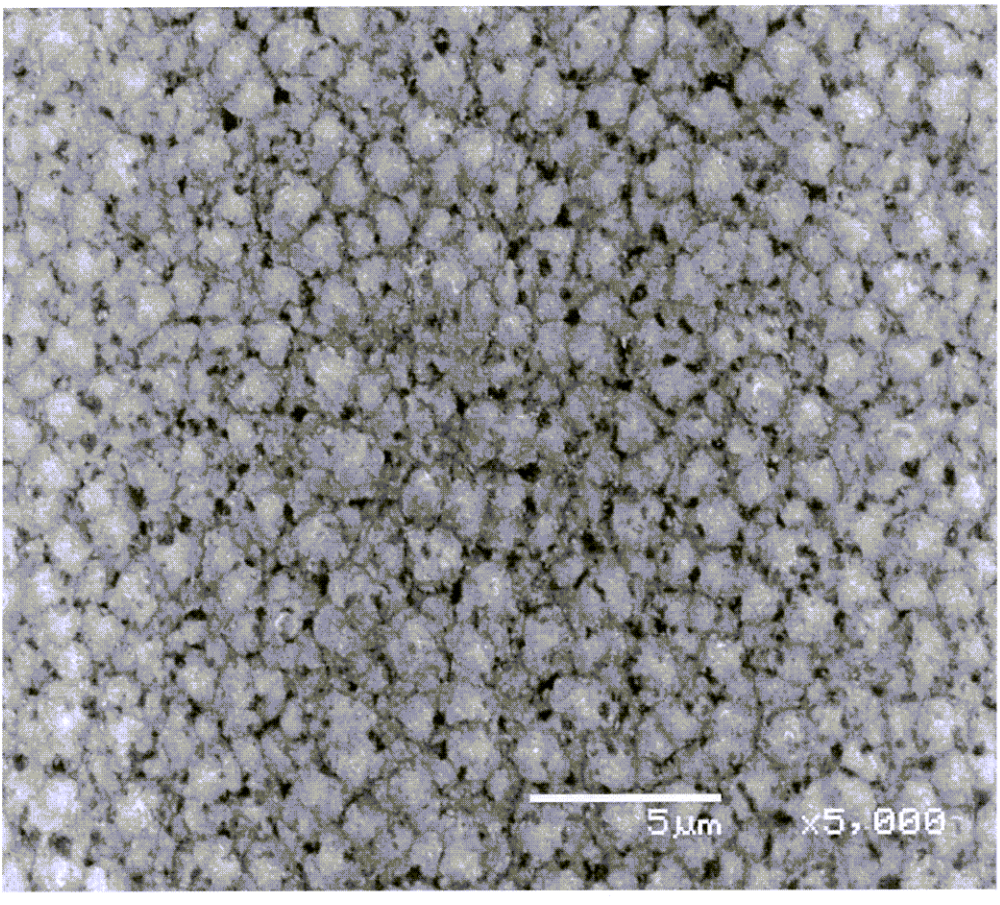

Figure 6b

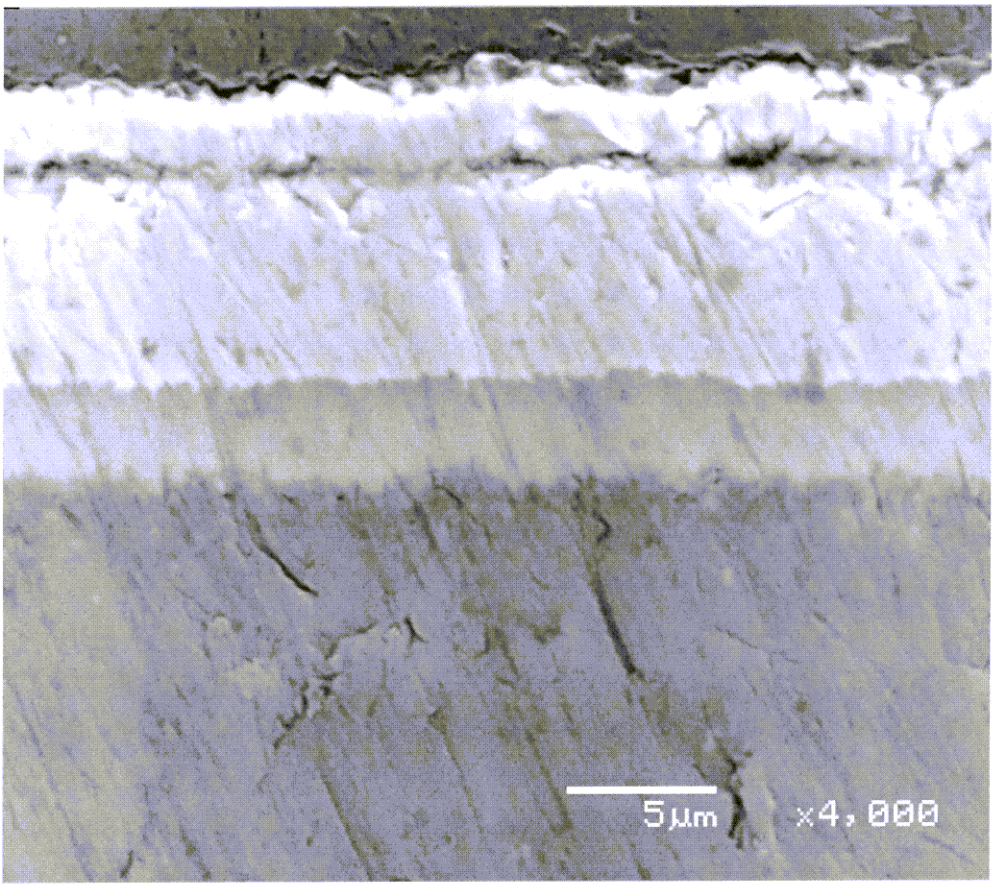

Figure 7a

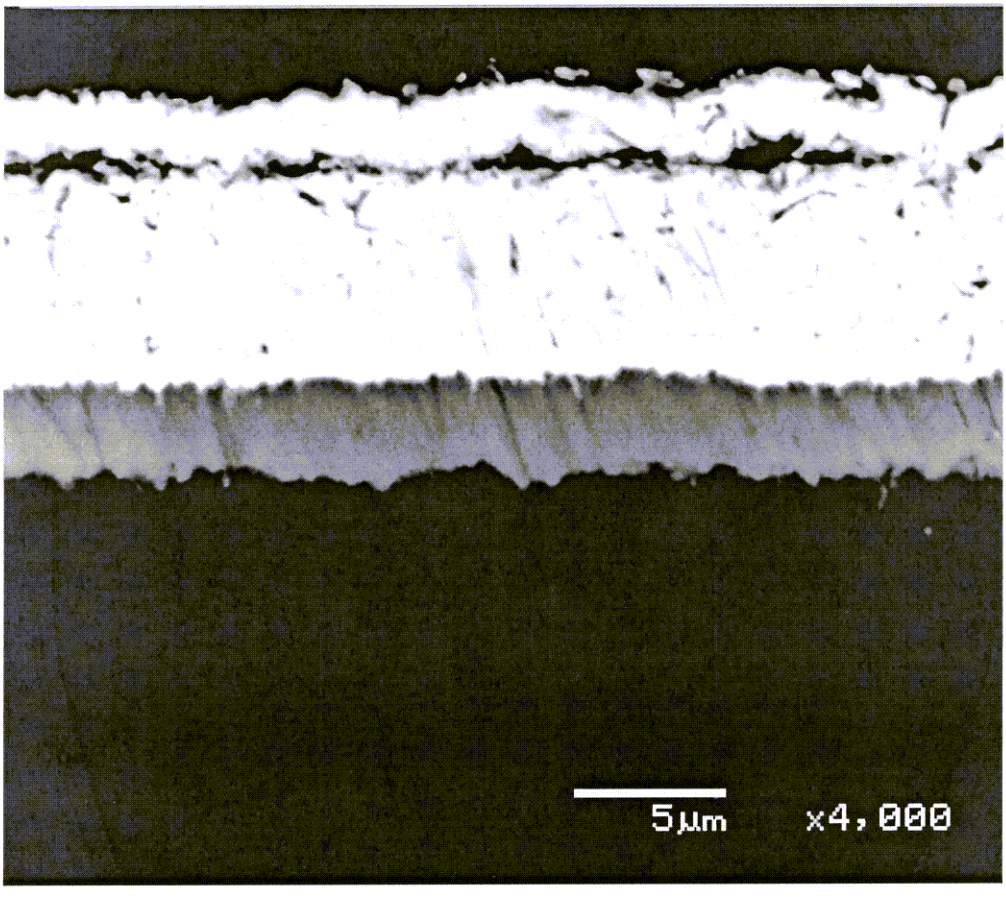

Figure 7b

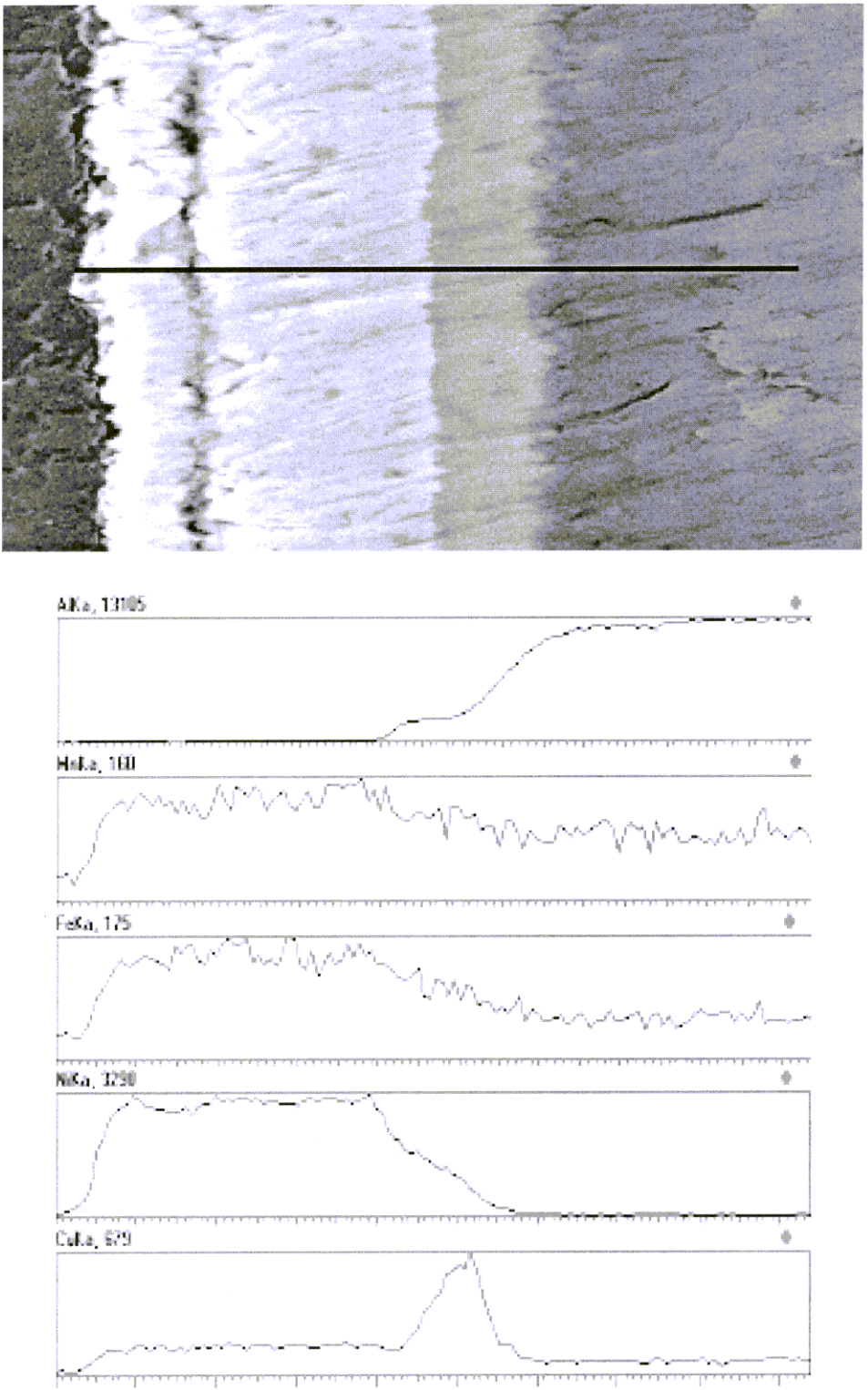

Figure 8

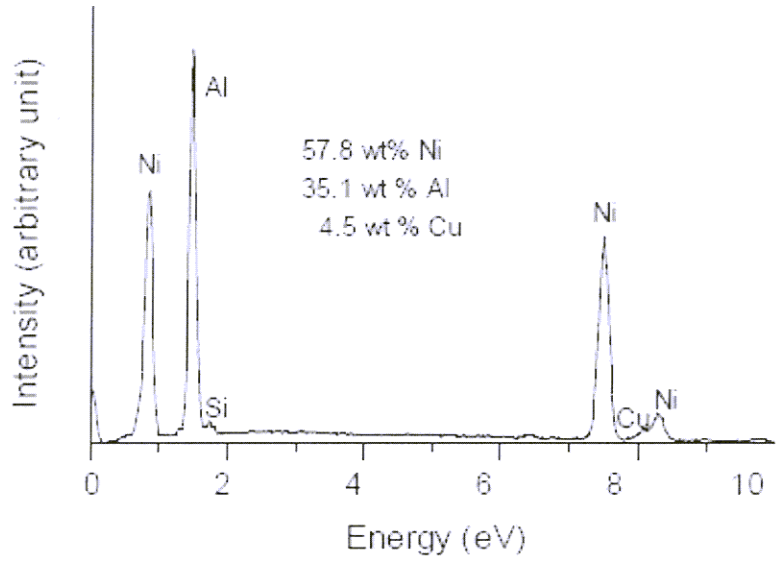

Figure 9a

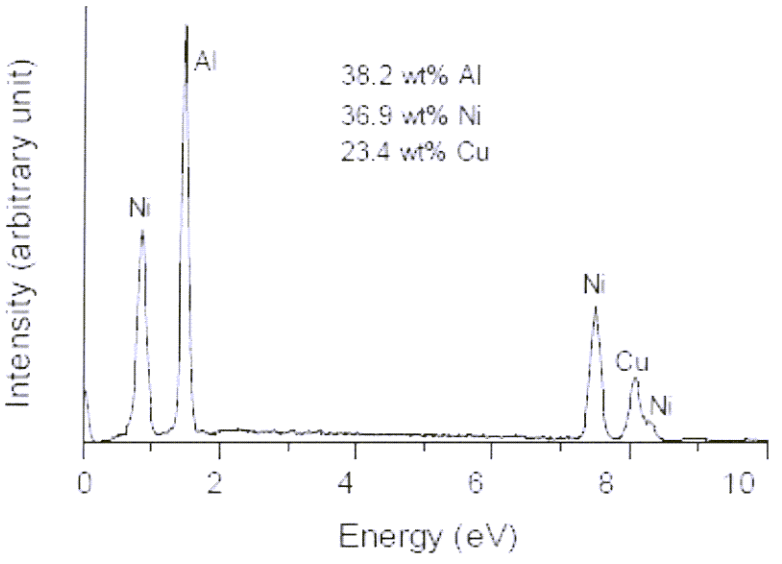

Figure 9b

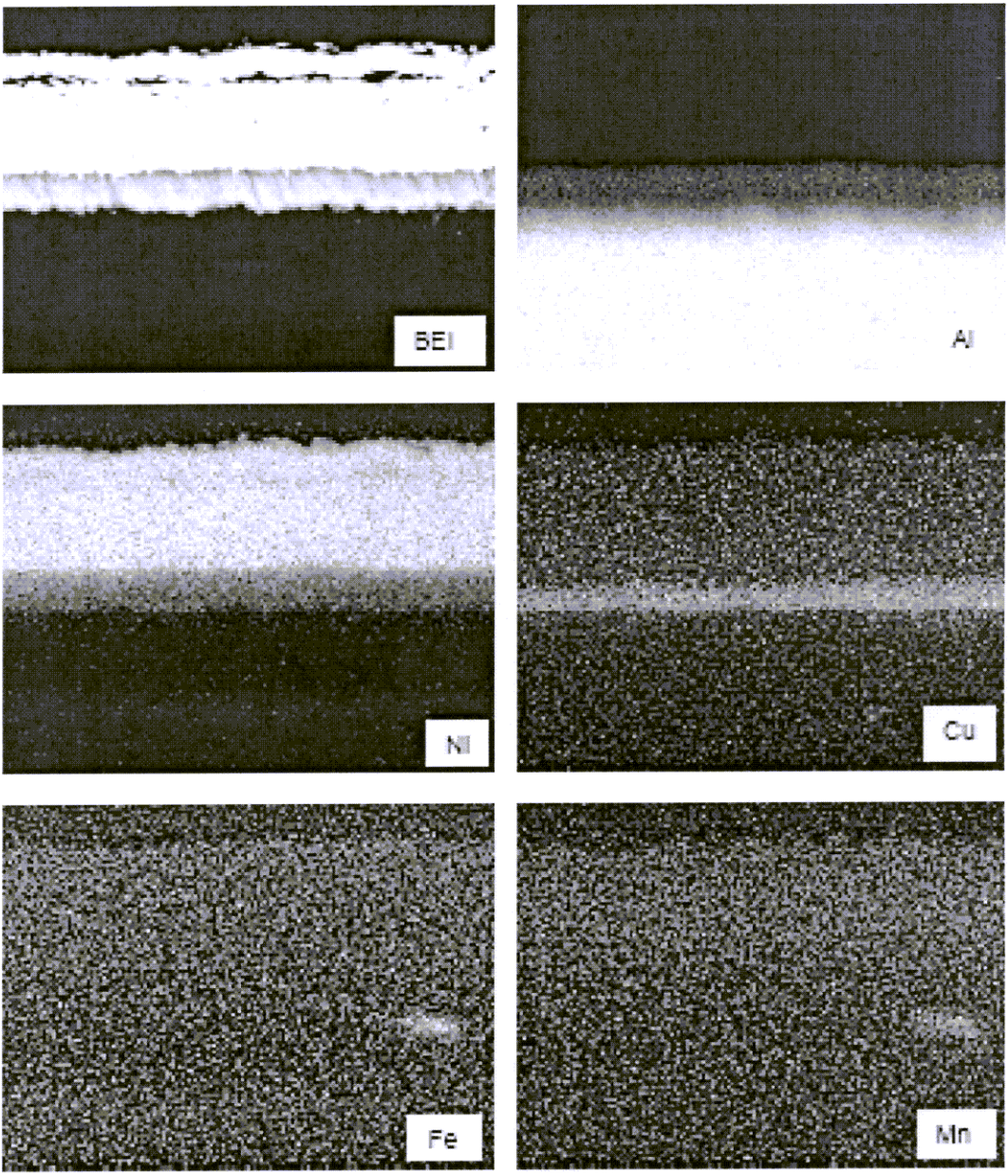

Figure 10

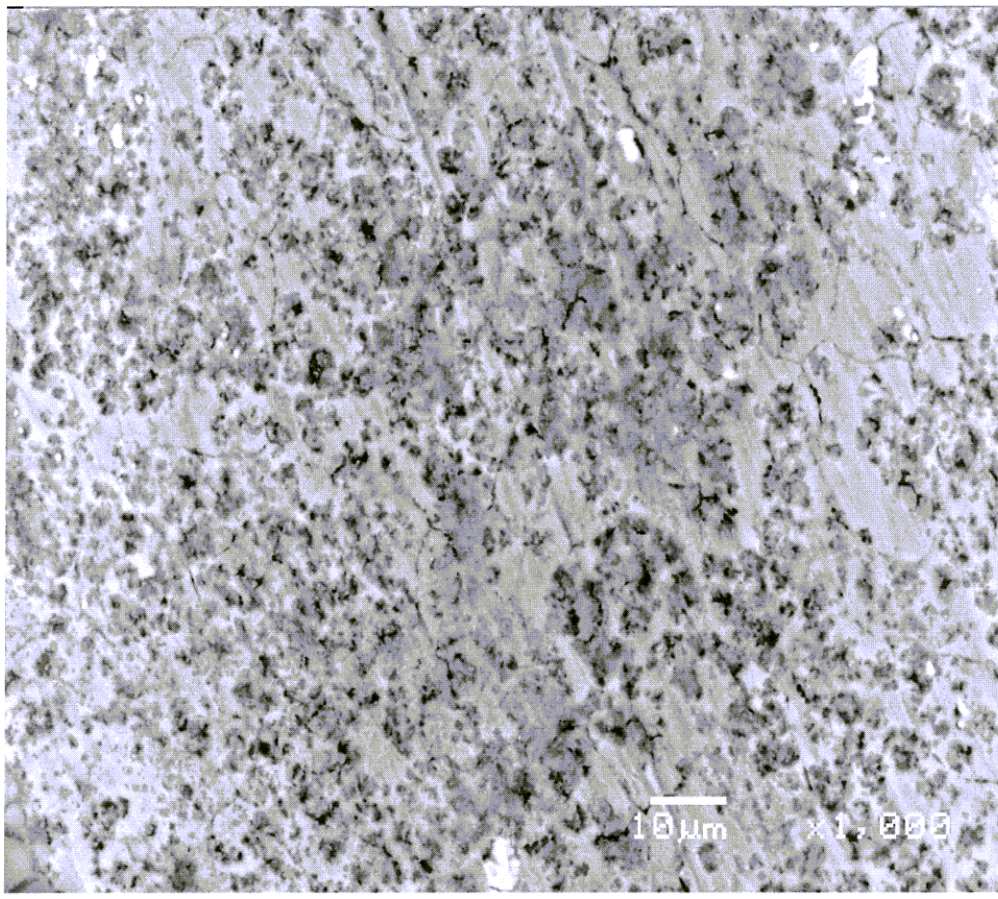

Figure 11a

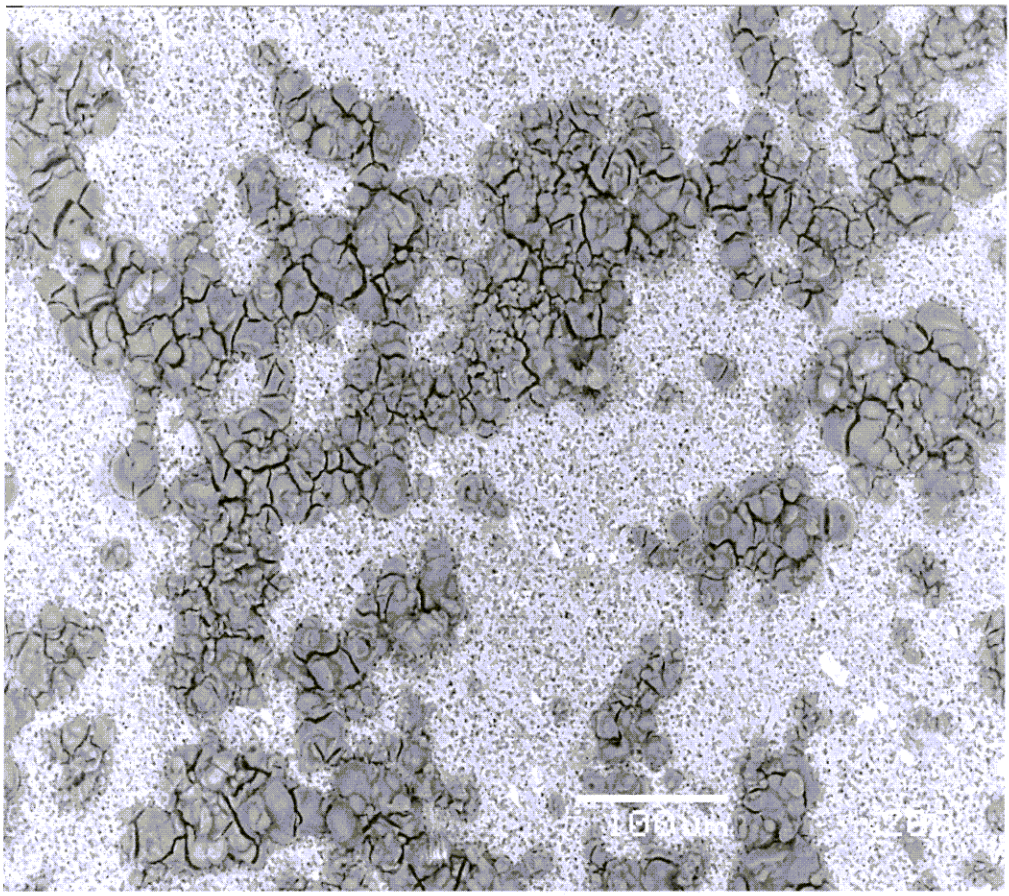

Figure 11b

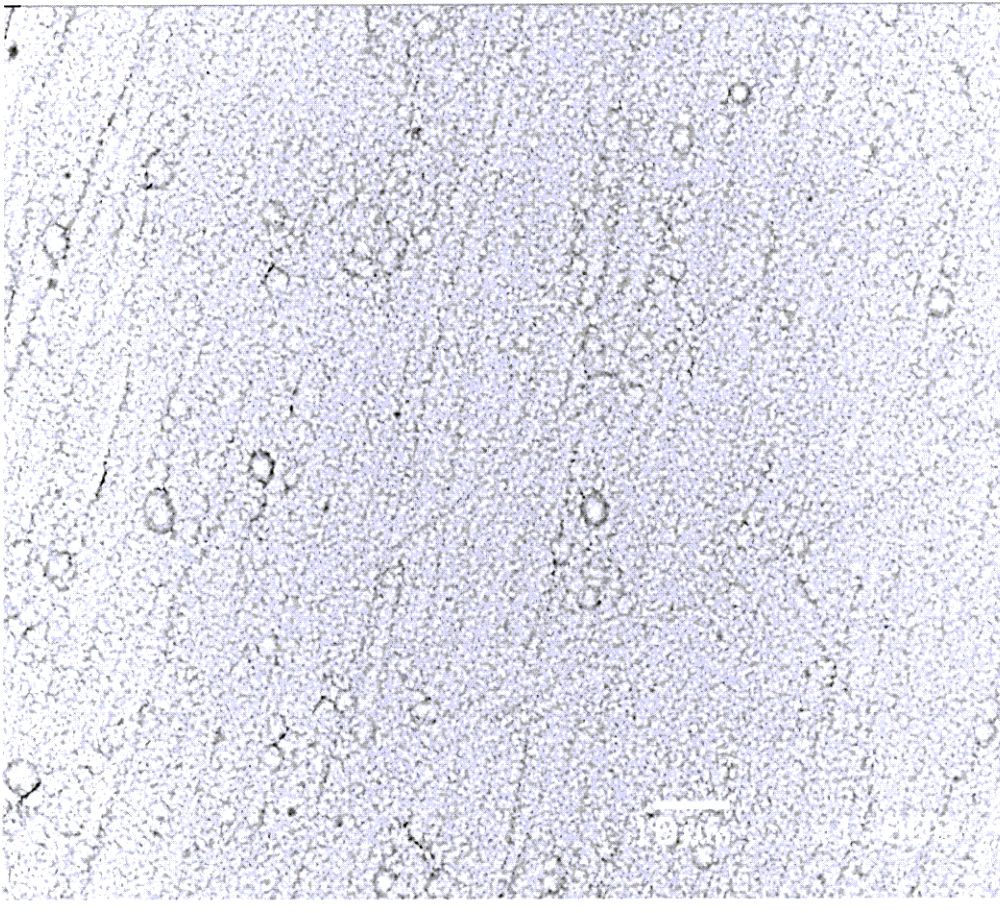

Figure 11c